Desalination and Water Treatment
www.deswater.com

doi: 10.5004/dwt.2019.23765

150 (2019) 386–395
May

Effect of cetyltrimethylammonium bromide on the biosorption of Acid Blue 25 onto Bengal gram fruit shell

L. Sivarama Krishna[a,b,*], K. Soontarapa[a,b,*], N.K. Asmel[c], A. Yuzir[d], W.Y. Wan Zuhairi[e]

[a]*Department of Chemical Technology, Faculty of Sciences, Chulalongkorn University, Pathumwan, Bangkok, 10330, Thailand, emails: svurams@gmail.com (L. Sivarama Krishna), Khantong.S@chula.ac.th (K. Soontarapa)*
[b]*Center of Excellence on Petrochemical and Materials Technology, Chulalongkorn University, Pathumwan, Bangkok, 10330, Thailand*
[c]*Building and Construction Technology Engineering, Northern Technical University, 41002 Mosul, Iraq, email: nabeelasmeel@yahoo.com*
[d]*Department of Environmental Engineering and Green Technology (EGT), MJIIT- Universiti Teknologi Malaysia, Jalan Sultan Yahya Petra, 54100 Kuala Lumpur, email: muhdaliyuzir@utm.my*
[e]*Geology program, School of Environmental Science and Natural Resources, FST, University Kebangsaan Malaysia, Bangi-43600, Selangor, Malaysia, email: wanzuhairi@yahoo.com*

Received 12 May 2018; Accepted 8 January 2019

ABSTRACT

This study explores an intensive investigation of the effect of cationic surfactant, cetyltrimethylammonium bromide (CTAB) on biosorption of Acid Blue 25 (AB25), an anionic dye, onto Bengal gram fruit shell (BGFS) from aqueous solution. The BGFS was characterized using Fourier transform infrared spectroscopy and scanning electron microscopy. Effect of AB25 and CTAB concentrations, time and temperature, were explored. The dye uptake by the BGFS was increased with increasing initial dye concentration up to 100 mg L^{-1}. The inclusion of 0.9 mmol L^{-1} of CTAB in the biosorption medium was greatly improved for the removal of AB25. The AB25 uptake was better described by the Langmuir adsorption model than the Freundlich model. This study shows that the maximum uptake of AB25 dye by BGFS in the absence of surfactant was evaluated and found 29.4 mg g^{-1}. Also, the results of this investigation revealed that the presence of 0.9 mmol L^{-1} CTAB in the biosorption medium increased the maximum uptake of AB25 to 166.6 mg g^{-1}, which is 5.7 times higher than the uptake capacity in the absence of CTAB. The biosorption kinetics was correctly described by the pseudo-second-order kinetic model for all cases studied a confirmation that a chemisorption process controlled the biosorption rate. Thermodynamic parameters ($\Delta H°$, $\Delta S°$, and $\Delta G°$) were determined for the biosorption of AB25 onto BGFS-CTAB. The biosorption process describes that the reaction was exothermic and spontaneous processes.

Keywords: Biosorption; Bengal gram fruit shell; Acid Blue 25; Cetyltrimethylammonium bromide

1. Introduction

Water pollution, as a result of swift industrialization, is of great concern globally. Wastewater contaminated with dyes is discharged into the environment or water bodies by various industries such as paper, textile, plastics, leather, pharmaceuticals, pigments, and cosmetics. Large quantities of wastewater contain high dyes concentrations, which are above the permissible limit. Several physical and chemical methods are studied for the remove these dyes from wastewater. The treatment methods include ion exchange, oxidation, reverse osmosis, electrochemical, biological, coagulation, and flocculation [1]. Comparing these techniques, adsorption is certainly superior to other methods because it is economical

* Corresponding authors.

and efficient. In the same way, biosorption was characterized by high efficiency, selectivity, cost-effectiveness, easy and possible regeneration, high removal capacity, low cost, and availability of biomaterials [2].

Textile industries release a different kind of dyes into water bodies. These dyes are generally toxic and can cause many health problems, such as nausea, vomiting, eye injury, and methemoglobinemia, in human beings. Dye molecules interfere with light penetration in water and interrupt biological processes. Similarly, some dye compounds are degraded into a variety of compounds that have toxic effects on aquatic organisms and mammals [3–5].

Different adsorbents have been discovered and utilized for the removal of color from wastewater. Activated carbon is popular among these adsorbents because it is efficient in decolorizing dyes, however costly. Many biological materials especially agricultural residues such as jujube seeds [1], walnut shell [6], kenaf core fibers [7], wheat straw [8], rice husk [9], spent rice biomass [10], hazelnut shells, wood sawdust [11], corn cob [12] and plum kernels [13], tea waste [14], spent green tea leaves [15], pineapple leaf powder [16], by low-cost adsorbents review [17] have been recently employed as carbon precursors for the removal of dyestuff from aqueous solutions.

Large quantities of Bengal gram (*Cicerarientinum Linn*) fruit shell biomass (BGFS) are annually produced as an agricultural by-product in some parts of the world. The cell walls of BGFS contain lignin, cellulose, and hemicelluloses. The shell of Bengal gram fruit is considered as waste biomass and readily available biosorbent. Thus, in the present investigation, this material was effectively tested for removal of Acid Blue 25 (AB25) dye from aqueous solutions. In our previous study, BGFS was successfully utilized to remove Congo red from wastewater [18]. Also, this study aims to investigate the biosorption behavior of Cetyltrimethylammonium bromide-Bengal gram fruit shell (CTAB-BGFS) toward AB25 dye and to compare the biosorption efficiency of CTAB-BGFS with that of BGFS. The AB25 dye, which was extensively used in the dyeing industry, is anionic in nature. To optimize the influence of operating factors such as surfactant concentration, dye concentration, and temperature, this study was focused on evaluating the kinetics and thermodynamics parameters on adsorption process.

2. Materials and methods

2.1. Preparation of BGFS bio-sorbent

The Bengal gram plant belongs to the class *Magnoliopsida*, order *Rosales*, family *Leguminosae*, and its botanical name are *Cicer arientinum Linn*. The fruit shells or pod coats of Bengal gram were collected in the agricultural fields in Parumanchala, Andhra Pradesh, India, during the harvesting season. The preparation methods for BGFS were already reported in our previous work [18]. In brief, Bengal gram fruit shell was washed thoroughly with distilled water to remove dirt and mud and dried for 24 h under sunlight. The dried material was ground to fine powder. The fine ground powder was passing through 53 μm sieve and the particle size, <53 μm was prepared for the experimental studies. This material was labeled as BGFS and used as biosorbent for removal of AB25 dye from aqueous solutions.

The BGFS having some major metal oxides such as SiO_2-0.2457%, Al_2O_3-0.1598%, Fe_2O_3-0.3008%, CaO-4.8598%, MgO-0.5452%, SO_3-0.4042% Na_2O-0.0658%, K_2O-5.3298, TiO_2-0.0846 %, MnO-0.0376%. The BGFS LOI and gross calorific value (GCV) were 87.89 and 4,128 (kcal kg^{-1}), respectively. The BGFS pHpzc is 4.75. The elemental analysis reports showed that the BGFS contains 39.21% of carbon, 5.71% of hydrogen, and 0.085% of nitrogen.

2.2. Preparation of AB25 solution and surfactant solutions

Acid Blue 25 (C.I. Acid Blue 25, chemical formula: $C_{20}H_{13}N_2NaO_5S$, molecular weight: 416.38, dye content: 45%) and cetyltrimethylammonium bromide (CAS Number 57–09–0, chemical formula: $CH_3(CH_2)_{15}N(Br)(CH_3)_3$, molecular weight: 364.45, assay: ≥99%) were purchased from M/S Sigma-Aldrich Chemicals and used as supplied. A 1,000 mg L^{-1} (stock solution) of AB25 dye was prepared using double distilled water, and diluted concentrations of AB25 for experimental work were prepared by diluting the stock solution. The concentration of AB25 was determined by measuring the absorbance of various concentrations of AB25 solutions at λ_{max} of 610 nm using a Chemito spectrophotometer. A 100 mmol L^{-1} (stock surfactant solution) was prepared from Cetyltrimethylammonium bromide (CTAB, $C_{18}H_{16}O_{12}N_4S_3$) by weighing and dissolving the calculated amount of CTAB in double distilled water.

2.3. Sorption experiments

Sorption experiments were carried out by adding 25 mL of AB25 and 200 mg of BGFS, in the presence of 0.9 mmol L^{-1} CTAB of concentration, in a 50 mL screw type Erlenmeyer flask at 35°C (room temperature). The mixture was agitated in a Julabo water bath shaker at 180 rpm. The residual concentration of AB25 was determined spectrophotometrically by taking the absorbance on Chemito UV-Visible spectrophotometer at 610 nm. The pH values of AB25 solutions were measured using a pH meter (Systronics pH system 361 Model). After equilibration at pre-determined time intervals, the samples were withdrawn from the shaker, and the AB25 solutions were separated from the BGFS by centrifugation for 20 min at 10,000 rpm. The absorbance of the supernatant solution was measured, and the amount of AB25 biosorbed was calculated.

The amount, q_t (mg g^{-1}), of AB25 biosorbed by BGFS at time t and was calculated using Eq. (1).

$$q_t = \frac{\left[\left(C_o - C_t\right)\cdot V\right]}{W} \tag{1}$$

In Eq. (1) C_o and C_t (mg L^{-1}) are the initial concentration and concentration at time t, respectively; V (L) is the volume of AB25 solution, and W (mg) is the mass of BGFS used.

The removal percentage of AB25 onto BGFS was evaluated using Eq. (2).

$$\%\ \text{Removal} = \frac{(C_o - C_e)}{C_o} \cdot 100 \quad (2)$$

where C_e (mg L^{-1}) is the equilibrium concentration of AB25 in solution.

2.4. Kinetic experiments

The kinetic experiments were investigated by varying the initial concentration of AB25 between 25 and 100 mg L^{-1} and keeping the surfactant concentration constant at 0.9 mmol L^{-1} for each set of the experiments.

2.5. Dependence on temperature

The effects of temperature on the removal of AB25 in the absence and presence of CTAB were studied at 35°C, 45°C, 55°C and 65°C. In this study, 25 ml of AB25 and CTAB (0.9 mmol L^{-1}) solution of 50 mg L^{-1} were added in a screw type Erlenmeyer flask and agitated at 180 rpm with 200 mg of BGFS (<53 μm) at different temperatures). The samples were withdrawn from the shaker at time intervals, and the AB25 solution was separated from the biosorbent by centrifugation for 20 min at 10,000 rpm. The absorbance of the residual dye solution was measured while the amount of AB25 biosorbed was evaluated using Eq. (1).

2.6. Influence of CTAB concentration on Acid Blue 25 removal

To study the influence of CTAB concentration on the removal of AB25 at initial pH of the dye, an optimization study was conducted with different CTAB concentration varied between 0 and one mmol L^{-1} while the initial AB25 concentration (50 mg L^{-1}) was kept constant. The flasks were continuously agitated in a shaker at 180 rpm constant shaking rate for 1 d for proper equilibration. The samples were withdrawn from the thermostated shaker and the AB25 solution was separated from the biosorbent by centrifugation at 10,000 rpm for 20 min. The absorbance of the supernatant solution was measured, and the amount of AB25 biosorbed was calculated using Eq. (1).

2.7. Surface characterization of BGFS

The Fourier transform infrared (FTIR) spectra were recorded in the transmission mode with a Thermo Nicolet, Nexus 670 Spectrometer infrared spectrometer. The powder samples were ground with KBr and compressed into a pellet. The FTIR spectra range between 4,000–400 cm^{-1} with resolution 4 cm^{-1} using the KBr disk technique were recorded in order to investigate the nature of the chemical bonds formed. Scanning electron microscopy (SEM) (Hitachi S-3000N) was used to investigate the morphology of the samples surfaces.

3. Results and discussion

3.1. Biosorbent characterization

Fig. 1 shows the FT-IR spectra of BGFS, BGFS-CTAB, and BGFS-CTAB-AB25. The slight variation in the transmittance

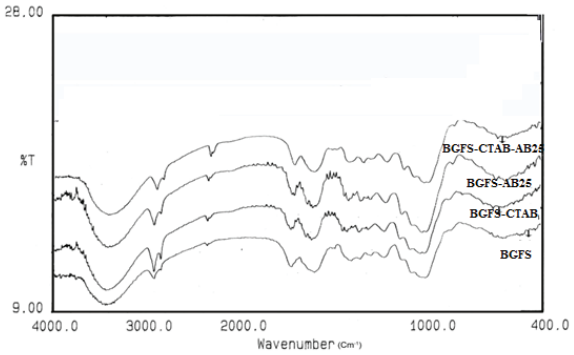

Fig. 1. FT-IR spectra of BGFS, BGFS-CTAB, BGFS-AB25 and BGFS-CTAB-AB25.

of the radiation was observed for all the samples (BGFS, BGFS-CTAB, and BGFS-CTAB-AB25) for the functional bonds OH stretch, CH_2–H stretch and C=O stretch at 3,435–3,433, 2,920–2,922 and 1,738–1,736 cm^{-1}, respectively. The bands at 2,854 cm^{-1} were ascribed to C–H stretching vibration of CH_3 and CH_2 groups of the alkyl chain of quaternary ammonium molecules [19–21]. The interaction of BGFS, BGFS-CTAB, and BGFS-CTAB-AB25 were confirmed by the appearance of new bands at 1,375–1,371 and 1,159–1,157 cm^{-1}, which correspond to the asymmetric bending vibrations of CH_2 and a C–O stretch of ester functional group. The key role of the two peaks observed in the FT-IR spectrum of BGFS-CTAB at 1,657 and 1,465 cm^{-1} corresponding to the C=O stretching of amide bond and C=C stretching was not observed in the spectra of BGFS and BGFS-CATB-AB25 [19,20]. The observation of appearance of the peaks at the above wavenumbers confirms on the BGFS surface covered with CTAB functional groups [21]. Similarly, the disappearances of the corresponding peaks in the BGFS-CTAB-AB25 were confirmed by the interaction of the AB25 with the polar end of CTAB. By this observation, the combination of BGFS with CTAB will be good for sorption of AB25 dye from the aqueous medium.

The SEM of BGFS, BGFS-CTAB, and BGFS-CTAB loaded with AB25-dye are shown in Figs. 2(a), (b), and (c), respectively. From this figures, it is seen that the BGFS and BGFS-CTAB surfaces show that BGFS possesses small particles and non-porous surface (Fig. 2(a)), however, the introduction of CTAB leads to the formation of large particles and coarse porous surface. This phenomenon becomes obvious with an increase of CTAB (Fig. 2(b)). This is an indication of the high probability of AB25 to be trapped and biosorbed. On the contrary, the surface of BGFS-CTAB-AB25 exhibited a rougher texture covered with the adsorbed AB25 dye molecules. The particles of AB25 dye-loaded BGFS-CTAB are larger because of biosorption of dye molecules on the surface (Fig. 2(c)).

3.2. Effect of CTAB concentration on the removal of Acid Blue 25

A 50 mg L^{-1} of AB25 dye was used to investigate the effect of CTAB concentration on the removal of AB25 dye; CTAB concentration was varied between 0 and 1 mmol L^{-1}.

The removal efficiencies of AB25 dye was enhanced from 13.6% to 75.7% with increases in CTAB concentration up to 1 mmol L^{-1}. The CTAB possesses a positively charged head group, and consequently, an increase in CTAB concentration increased the removal of anionic AB25 molecules as a result of electrostatic interaction [22].

Various concentrations of CTAB produced varying effects on the removal of oppositely charged anionic AB25. At a lower concentration of CTAB, relatively small pre-micellar aggregates, containing some CTAB molecules, were formed in the presence of the AB25, which resulted in lower dye removal. However, at higher surfactant concentration, complex dye-surfactant associates or aggregates, which led to very high dye uptakes, were formed. Increasing the CTAB concentration decreased the peak intensity (Fig. 3) and enhanced the biosorption capacity of AB25 from 13.6% to 75.7 %. Generally, CTAB has 0.9 mmol L^{-1} critical micelle concentration (CMC), afterward the surfactant molecules form aggregates. Therefore, in the present investigation, the optimum concentration of 0.9 mmol L^{-1} of CTAB was used for the further study (Fig. 4).

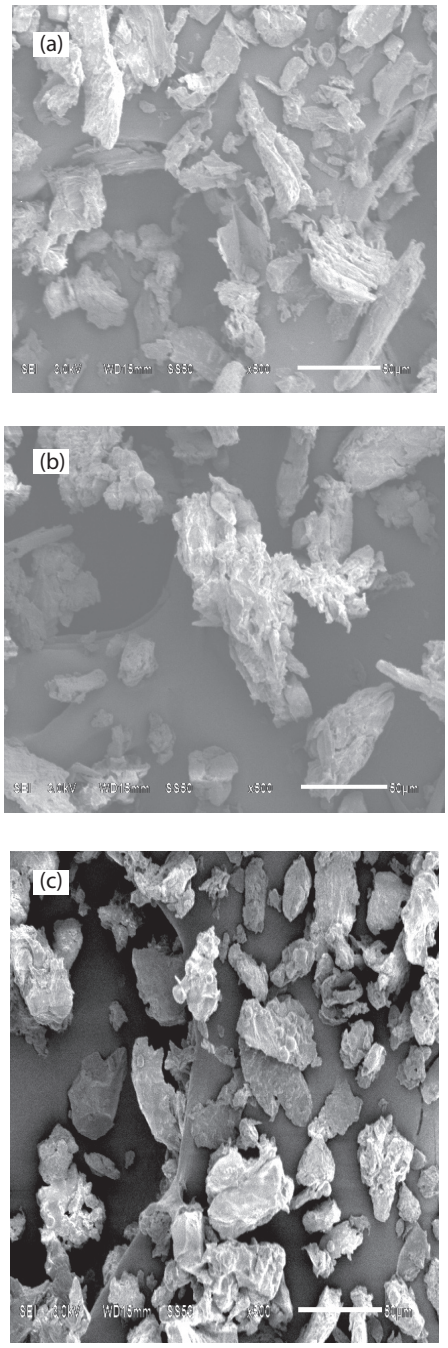

Fig. 2. SEM images of (a) BGFS, (b) BGFS-CTAB, and (c) AB25 dye loaded BGFS-CTAB.

3.3. Effect of initial AB25 concentration on biosorption, with or without 0.9 mmol L^{-1} of CTAB

The biosorption of AB25 on BGFS in the absence and presence of CTAB at 35°C was studied using different AB25 concentrations (25–100 mg L^{-1}). The AB25 dye biosorption was a function of AB25 concentration—a notable enhancement in the AB25 dye removal was observed in the presence of CTAB. The AB25 removal was fast at the first 60 min, after that the reaction proceeded at a slower rate and subsequently attained saturation. In the absence and presence of CTAB, the results indicate that at higher AB25 concentration, the uptakes of AB25 dye by BGFS were also higher.

When the initial AB25 concentration was increased from 25 to 100 mg L^{-1}, in the absence of surfactant, the equilibrium biosorption was increased from 2.07 to 7.69 mg g^{-1}. Similarly, in the presence of the surfactant, the removal

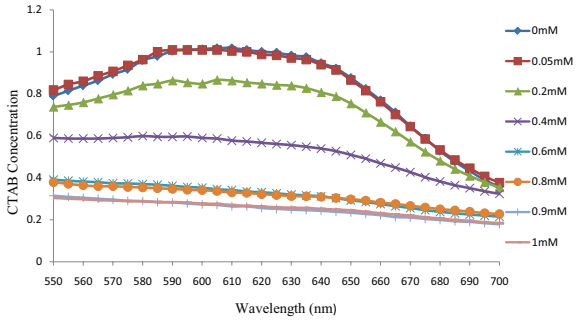

Fig. 3. Effect of CTAB concentration on AB25 removal.

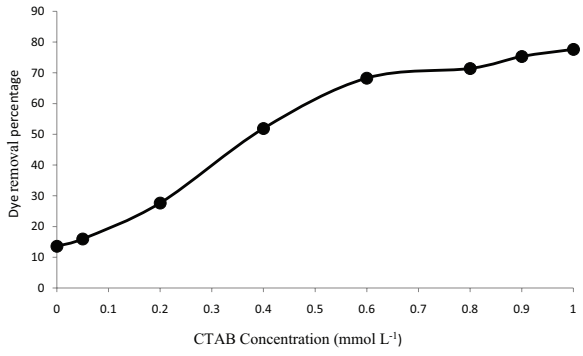

Fig. 4. Dye removal percentage at different concentration of CTAB.

efficiency of AB25 increased sharply from 2.82 to 11.36 mg g^{-1} when the initial concentration of the dye was increased from 25 to 100 mg L^{-1}. The effect of 0.9 mmol L^{-1} CTAB on the biosorption of AB25 onto BGFS at various initial dye concentrations is pronounced. At lower concentrations of the dye, the ratio of the concentrations of AB25 to BGFS sites was higher due to an increase in AB25 uptake. However, at higher dye concentrations lower biosorption yield as observed as because of the result of the saturation of biosorption sites. The AB25 reached equilibrium approximately at 45, 60, 90 and 120 min in both systems (with and without surfactant) for respective AB25 concentrations of 25, 50, 75 and 100 mg L^{-1}. The biosorption experiments, however, were carried out at 300 min to ensure observance of equilibrium conditions. Different data on the sorption kinetics of AB25, using various biosorbents showed a similar range of biosorption rates. Studies on the sorption of AB25 on hazel nutshell [11], spent brewery grains [23] and diatomite [24] also reported the equilibrium time of 300 min.

3.4. Biosorption kinetics of AB25 with and without 0.9 mmol L^{-1} CTAB

For adsorption technique, the kinetic study of adsorption is important because it gives useful insights into the reaction pathways and mechanisms of the adsorption process. The kinetics of AB25 dye was investigated to understand and interpret the behavior of the dye sorption onto the BGFS in the absence and presence of CTAB. For this reason, biosorption capacity (q_e) was plotted against time for various AB25 concentrations (in the absence and presence of surfactant). For surfactant concentration and time dependences; smooth, single, and continuous sorption curves were obtained. The extent of dye removal is a function of contact time for all the kinetic experiments investigated. Addition of CTAB strongly affects the sorption of AB25 (an anionic) dye, and biosorption capacity of the dye increased as time increases, in the presence of CTAB. In the absence of CTAB, the amount AB25 biosorbed at equilibrium onto BGFS was 32.6 mg g^{-1}, however, when 0.9 mmol L^{-1} of CTAB was included to the biosorption medium, the uptake of the dye increased to 42.5 mg g^{-1}. This percentage increment in biosorption capacity in the presence of CTAB is 30.4%. Removal of AB25 by BGFS was instantaneous; within the first 45 min, 57% of the total biosorbed amount of AB25 was removed, and an apparent equilibrium was attained within 4 h. This kind of rapid dye-uptake by BGFS is an indication that BGFS has an affinity for the AB25 dye, this phenomenon is physical adsorption, and the dye-uptake occurs mainly by surface binding. Though the inclusion of 0.9 mmol L^{-1} CTAB did not change the equilibrium time, only the sorption profile of the dye changed. There was a steady increase in the sorption of AB25 onto BGFS in the presence of CTAB (there was the uptake of 62.8% of total amount biosorbed within first 10 min), and amount biosorbed remained constant after an equilibrium time of 240 min. This slower type of biosorption process indicates that internal and external diffusions of the dye and dye-surfactant species control adsorption rate. From these results, the contact time for the rest of all the batch experiments was fixed at 300 min to attain equilibrium at all cases.

3.5. Application of pseudo-first-order and pseudo-second-order kinetic model

Sorption can be described as a time-dependent process. For sorption of dyes from wastewaters and aqueous solutions, it is therefore important to know the rate of sorption for biosorbent evaluation, operation control, and process design. Simplified pseudo-first-order and pseudo-second-order kinetic models were employed to fit the experimental data in the presence and absence of CTAB [25]. The pseudo-second-order model is the most commonly used model for the description of dyes sorption, and the model takes into consideration all sorption steps such as internal particle diffusion and external film diffusion as pointed out by McKay and Ho [26]. This model predicts the sorption behavior over the whole range of sorption period, which agrees with the chemisorption mechanism as the rate-determining step. The pseudo-second-order equation is established on the basis of the sorption capacity of the solid phase.

The linear forms of pseudo-first-order and pseudo-second-order are represented in Eqs. (3) and (4), respectively.

$$\log\left(q_e - q_t\right) = \log q_e - \frac{k_1}{2.303}\cdot t \tag{3}$$

$$\frac{t}{q_t} = \frac{1}{k_2 q_e^2} + \frac{1}{q_e}\cdot t \tag{4}$$

where k_1 (min^{-1}) and k_2 (g mg^{-1} min^{-1}) are the respective rate constants of pseudo-first-order and pseudo-second-order of biosorption process while q_e (mg g^{-1}) is the equilibrium amount of AB25 biosorbed on biosorbent.

Intra-particle diffusion was used to investigate the mechanism of the AB25 biosorption onto BGFS. For identification of the mechanism involved in the biosorption process, the intra-particle diffusion plot is always used. This is an empirical model, which is founded on the functional relationship common to most of the biosorption processes, where uptake is proportional to $t^{0.5}$ rather than the contact time t. The intra-particle diffusion, as proposed by Weber and Morris, is depicted by Eq. (5).

$$q_t = k_{\mathrm{pi}} t^{0.5} + C_i \tag{5}$$

The k_{ip} (mg g^{-1} $min^{-0.5}$) in Eq. (5) is the rate parameter of stage i, which is obtained from the slope of the straight line plot of q_t vs. $t^{0.5}$; the intercept of the plot gives C_i, which provides an insight about the thickness of the boundary layer.

The values of equilibrium uptake ($q_{e\mathrm{Exp}}$) and rate constant (k_2) were obtained from the linear plots of the pseudo-second-order model for all AB25 concentrations presented in Table 1. It was observed that the second-order rate constants were affected by the initial concentration of AB25 and the added CTAB (0.9 mmol L^{-1}). The rate constants, which diminished remarkably with increasing AB25 concentration in the absence and presence of a surfactant, could be attributed to the dominant surface sorption. The values of determination coefficients obtained were approximately

Table 1
Kinetic parameters for the biosorption of AB25 onto BGFS and BGFS-CTAB at different dye concentrations

System name	Variable values	$Q_{e,exp}$ (mg g^{-1})	Pseudo-first-order			Pseudo-second-order		
			$Q_{e,cal}$ (mg g^{-1})	k_1 (min^{-1})	R^2	$Q_{e,cal}$ (mg g^{-1})	k_2 (gm g^{-1} min^{-1})	R^2
BGFS-AB25	25	2.0703	2.2728	0.0081	0.9811	1.9850	0.2091	0.9985
Conc. (mg L^{-1})	50	4.0723	4.2052	0.0115	0.9697	4.0512	0.8777	0.9940
	75	5.7813	5.9448	0.0120	0.9678	5.7674	2.4131	0.9999
	100	7.6855	8.7915	0.0069	0.9877	7.5417	3.8402	0.9998
BGFS-AB25-CTAB	25	2.8193	3.0092	0.0092	0.9445	2.7881	0.8397	0.9995
Conc. (mg L^{-1})	50	5.7002	6.1135	0.0090	0.9889	5.6405	2.3191	0.9997
	75	8.5371	8.6277	0.0152	0.9678	8.5618	4.5249	0.9999
	100	11.3643	12.0755	0.0094	0.9761	11.2995	8.4388	0.9999

0.999, and good fittingness of experimental and theoretical q_e values for all combinations suggest the suitability of pseudo-second-order kinetic model in explaining the kinetics of AB25 biosorption onto BGFS. The values of equilibrium sorption capacities predicted by the model agreed with the values of experimental equilibrium dye uptake.

Pseudo-second-order and pseudo-first-order kinetic models could not explain the diffusion mechanism. The intra-particle diffusion model was therefore used to analyze the kinetic data. Weber and Morris model, presented in Eq. (5), was used to elucidate the intra-particle diffusion mechanism by making a plot of q_t vs. $t^{0.5}$. The plot would pass through the origin if the intra-particle diffusion were the only rate-controlled step, however, if not, the boundary layer diffusion controlled the biosorption process some to some extent. The plots of q_t vs. $t^{0.5}$ were not linear over the entire time range—an indication that the sorption process is affected by more than one process. From these plots, three linear regions (namely boundary layer diffusion, intra-particle diffusion in macro, meso and micro pores) were observed. The three segments are followed by horizontal lines representing the system at equilibrium.

The three linear regions could be explained as thus: at the start of biosorption process, there is a linear region, which represents the rapid surface loading; this is followed by the second linear region that represents pore diffusion; and a third and final horizontal linear region, which represents the equilibrium condition. The various regions in the graph and data of linear regressions for various initial concentrations were analyzed using the Microsoft Excel 2003® software package. The k_{ip} (intra-particle diffusion parameter) and boundary-layer thickness were evaluated from the respective slope and intercept of each region of the plot.

The correlation coefficients for the intraparticle diffusion model are also lower than the pseudo-second-order model, but this model indicates that an intraparticle diffusion model may follow the adsorption of AB25 onto BGFS-CTAB up to 90 min. The values of intercept give an idea about the boundary layer thickness such as the larger the intercept, the greater is the boundary layer effect. The intraparticle diffusion model values are shown in Table 2.

In the BGFS-CTAB system shows the higher intercepts indicated that the boundary layer effect could not be ignored for biosorption of AB 25. Since the K_{ip3} and K_{ip2} values were smaller than the K_{ip1} values, the intraparticle diffusion should be the limiting step for the biosorption of AB 25 onto BGFS-CTAB. All the intercepts calculated in the presence of CTAB and absence CTAB systems. In the presence of BGFS-CTAB were lower than in BGFS system, indicating a lateral interaction between the dye and BGFS-CTAB system is more suitable for the sorption studies.

3.6. Application of equilibrium models in the absence and presence of 0.9 mmol L^{-1} CTAB

Langmuir and Freundlich isotherm models, the most frequently employed two-parameter models as shown in adsorption literature, describe the sorption of dye molecules from the dye solution on the biomass. The empirical Langmuir equation is suitable for monolayer sorption onto a completely homogenous surface with the negligible interaction between the sorbed molecules and a finite number of binding sites. The Freundlich isotherm model, contrary to the Langmuir model, assumes neither limited levels of sorption nor homogeneous site energies. The earliest known empirical equation is the Freundlich model, and it is consistent with the exponential distribution of active centers, which is a characteristic of heterogeneous surfaces. The following equations represent both isotherms:

Langmuir isotherm model:

$$\frac{C_e}{q_e} = \frac{1}{Q_{max} K_L} + \frac{C_e}{Q_{max}} \tag{6}$$

where Q_{max} (mg g^{-1}) represents the maximum biosorption capacity of BGFS, and K_L (L mg^{-1}) represents the Langmuir constant, which is related to the biosorption energy.

Freundlich isotherm model:

$$\log q_e = \log K_F + \frac{1}{n} \log C_o \tag{7}$$

where K_F denoted the Freundlich constant while $1/n$ is the heterogeneity factor.

To investigate the effect of surfactant on AB25 sorption, the Freundlich and Langmuir equations were applied to the equilibrium data. The curvilinear relationship between the residual concentration of AB25 at equilibrium and the amount of AB25 biosorbed per unit weight of biomass implies that saturation of binding sites took place at the higher concentrations of AB25, both in the presence and absence of 0.9 mmol L^{-1} CTAB. From the plots, it was shown that the equilibrium sorption of AB25 was enhanced by the addition of 0.9 mmol L^{-1} CTAB, and the influence of 0.9 mmol L^{-1} CTAB cationic surfactants on AB25 uptake was prominent.

The fitting parameters of Langmuir and Freundlich for AB25 sorption are presented in Table 3. The suitability of these models was established from the determination coefficient (R^2) of the fitted curves. The determination coefficients for the Langmuir and Freundlich models are in the range 0.9913–0.9999 and 0.9960–0.9967, respectively. Thus it indicates that better fits were obtained for the Langmuir model compared with the Freundlich model in the presence of CTAB. It was also shown from the data that the Langmuir model gave a close prediction of the equilibrium data; this is evident from the overlapping of its model curves. These results suggest that BGFS-CTAB presents homogeneous adsorption sites and that the interaction of the dye on BGFS-CTAB biomass. The constants of the adsorption models express the affinity of the biosorbent and surface properties and were used to compare the adsorptive capacity of BGFS for AB25. The Freundlich constant n (an empirical parameter) varies with the level of heterogeneity indicating the degree of nonlinearity between unabsorbed AB25 concentration and AB25 uptake capacity and related to the distribution of bonded ions on the sorbent surface. Generally, $n > 1$ signifies that adsorbate is favorably biosorbed on a biosorbent; the higher the value of n, the stronger the biosorption intensity. For the equilibrium experiments in the presence of 0.9 mmol L^{-1} CTAB, the value of n, which is higher than unity, is an indication that AB25 molecules are favorably biosorbed onto BGFS. The value of n is also a proof that the biosorption intensity of AB25 was positively affected by the 0.9 mmol L^{-1} CTAB. The K_F is the sorption coefficient, which is also related to biosorption capacity; this constant represents the quantity of adsorbed AB25 for a unit equilibrium concentration. A higher value (1.18) of K_F was obtained in the absence of CTAB, and this value decreased to 0.9424 in the presence of 0.9 mmol L^{-1} CTAB; this agrees with the experimental observation. The parameters (Q_{max} and K_L) of the Langmuir model, presented in Table 3, also indicates that sorption of AB25 was largely depended on the CTAB added. Although the Freundlich model fails to explain the saturation behavior of the biosorbent, it gives Q_{max} value, which represents the monolayer saturation at equilibrium or the total capacity of BGFS sorbent for AB25 dye. High Q_{max} values indicate high capacity binding for AB25 in the presence of surfactant. The BGFS exhibits maximum sorption capacity (Q_{max}) in the presence of 0.9 mmol L^{-1} CTAB, as shown in Table 3. Addition of 0.9 mmol L^{-1} CTAB dramatically increased the maximum capacity of the biomass to remove AB25 from 29.41 to 166.67 mg g^{-1}. The high value of K_L denotes a steep beginning of the isotherm that reflects high affinity of BGFS for AB25. Similarly, the high value of K_L obtained in the presence of CTAB also signifies its positive effect for AB25 removal. The parameters of the isotherms successfully described the experimental data and gave useful information about the maximum sorption capacity (Q_{max}), relative sorption capacity (K_F), the nature and affinity of the adsorbents for AB25 (in the absence and in presence of surfactant systems).

Table 2
Intraparticle diffusion model

Linear portion	Constants	Variables							
		Concentration (mg L^{-1})				Temperatures (°C)			
		25	50	75	100	35	45	55	65
First	K_{P1}	0.0285	0.0314	0.101	0.0885	0.0314	0.0647	0.0468	0.0483
	C_1	2.3264	4.9704	7.3817	10.305	4.9704	5.0110	5.0827	5.2439
	R^2	0.9743	0.9801	0.9723	0.9958	0.9801	0.9908	0.8185	0.9661
Second	K_{P2}	0.0264	0.0181	0.013	0.0422	0.0181	0.0111	0.0116	–0.0778
	C_2	2.3641	5.1944	8.3078	10.63	5.1944	5.3748	5.3165	5.9341
	R^2	0.9891	0.9651	0.9882	0.9871	0.9651	0.9901	0.9912	0.9566
Third	K_{P3}	–	0.0401	–	–	0.0401	–	–	–0.0419
	C_3	–	5.0107	–	–	5.0107	–	–	5.0691
	R^2	–	0.9807	–	–	0.9807	–	–	0.9955

Table 3
Application of equilibrium models

System	Variables	Langmuir constants				Freundlich constants			
	(mg L^{-1})	Q_{max}(mg g^{-1})	K_L(L mg^{-1})	R^2	χ^2	K_F	n	R^2	χ^2
BGFS-AB25	Conc.	29.41	0.0090	0.9913	0.0149	1.1779	0.3439	0.9967	0.0142
BGFS-CTAB-AB25	Conc.	166.67	0.0080	0.9999	0.0492	0.9424	1.1246	0.9960	0.0809

3.7. Error analysis

An error is required to evaluate the fit of the experimental equilibrium data to an isotherm equation. The coefficient of determination (R^2) and a nonlinear Chi-square test were performed for the linear forms of Langmuir and Freundlich isotherm models used in this study. The sum of the squares of the differences between the experimental data and the theoretical data obtained from models, with each squared difference divided by the corresponding data calculated using the models, gives the Chi-square test statistics. The Chi-square is represented mathematically by Eq. (8).

$$\chi^2 = \frac{\sum\left(q_e - q_m\right)^2}{q_m} \tag{8}$$

where q_m is the theoretical equilibrium capacity obtained from the model (mg g^{-1}) and q_e is the experimental equilibrium capacity (mg g^{-1}). The χ^2 will be a small number if the experimental and theoretical data are similar, however, if the data are different, χ^2 will be a big number. It is, therefore, necessary to analyze the data using the non-linear Chi-square test to ascertain the best-fit isotherm model for sorption system.

Table 3 presents the results of the application of correlation coefficients (R^2) and non-linear Chi-square test (χ^2) of the equilibrium capacity (q_e) for two adsorption isotherms. Freundlich model gave the best fit for biosorption of AB25 onto BGFS, with the highest R^2 of 0.9967 and lowest χ^2 of 0.0142 for data in the absence of CTAB. In the presence of CTAB, the Langmuir model had the highest R^2 of 0.9999 for AB25 biosorption onto BGFS and low χ^2 of 0.0492—signifying that adsorption of AB25 onto BGFS in the presence of CTAB is homogeneous. As shown in Table 3, the Langmuir isotherm model has higher determination coefficient values and lowest Chi-square (χ^2) values in this study.

4. Thermodynamic parameter

The thermodynamic parameters such as Gibbs free energy (ΔG^o), enthalpy (ΔH^o) and entropy (ΔS^o) were calculated to evaluate the effect of temperature on sorption process of AB25 onto BGFS-CTAB using Eqs. (9)–(11).

$$\Delta G° = -RT \ln K_c \tag{9}$$

where

$$K_c = \frac{C_s}{C_e} \tag{10}$$

$$\ln K_c = \frac{\Delta S°}{R} - \frac{\Delta H°}{RT} \tag{11}$$

where C_s represents the equilibrium concentration of AB25 on biosorbent; C_e (mg L^{-1}) represents the equilibrium concentration of AB25 dye in solution, K_c is the adsorption distribution coefficient; R (8.314 J mol^{-1} K^{-1}) represents the ideal gas constant, and T (K) is the sorption temperature.

Table 4 presents the thermodynamic parameters of the biosorption of AB25 onto BGFS. The biosorption process is feasible and spontaneous because $\Delta G°$ has negative values. Generally, the values of energy $\Delta G°$ in the range of 0 and –20 kJ mol^{-1} indicate that the sorption process is physical sorption while the values in the range of –80 and –400 kJ mol^{-1} signify chemisorption [12]. The values of energy $\Delta G°$ obtained in this study suggest that the biosorption process follow physical sorption. Since $\Delta H°$ has a negative value, it is safe to conclude that the biosorption process is exothermic, implying that the process is stable energetically. The $\Delta S°$ has negative values, which reflect a decrease in randomness at the solid/solution interface during the sorption process.

5. The mechanism of enhanced biosorption capacity of AB25 on BGFS-CTAB

To further explain the mechanism of enhanced biosorption capacity of BGFS-CTAB, the effect of the amount of surfactant on biosorption capacity of BGFS for AB25 at dye initial pH 6.95 was compared. The experimental q_e of BGFS and BGFS-CTAB increased as the concentration of the surfactant used in the modification process was increased. Obviously, the amount of surfactant modified onto BGFS will increase with an increase in the concentration of surfactant used in the modification process. Therefore, the amount of quaternary ammonium cation on BGFS surface increases the cations, which results in increasing of electrostatic attractions between anionic AB25 dye and biosorbent. Besides, the biosorption capacities of BGFS and BGFS-CTAB for AB25 are 29.4 and 166.6 mg g^{-1}, respectively. These results indicate that more CTAB surfactants were fixed on BGFS surface and the cationic head group was free. The higher biosorption capacity of BGFS-CTAB is mainly due to the strong electrostatic attractions between the negatively charged group (SO_3^-) of dye molecule and free quaternary ammonium cation. Biosorption structure shown in Fig. 5 gives a better illustration of the biosorption process.

Table 4
Thermodynamic parameters

System	Temperatures (°C)	log*Kc*	$\Delta G°$ (kJ $mole^{-1}$)	$\Delta H°$(kJ $mole^{-1}$)	$\Delta S°$(kJ $mole^{-1}$ K^{-1})
BGFS-AB25-CTAB	35	1.0157	–5.9898	–31.1140	–0.0816
	45	0.9087	–5.5328		–0.0804
	55	0.8750	–5.4954		–0.0781
	65	0.5576	–3.6088		–0.0814

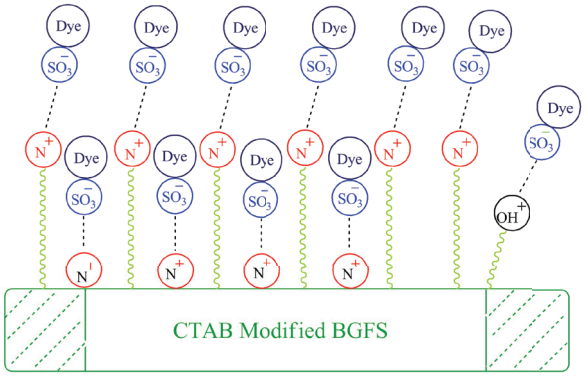

Fig. 5. Mechanism of Acid Blue 25 dye removal.

Table 5
Comparison of various low-cost adsorbents

S. No.	Adsorbent	Adsorption capacity q_e (mg g^{-1})	Reference
1	*BGFS-CTAB*	*166.67*	*Present study*
2	*BGFS*	*29.41*	*Present study*
3	Hazelnut	40.80	[11]
4	Walnut	36.98	[11]
5	Cherry	31.98	[11]
6	Oak	27.85	[11]
7	Pitch-pine	26.19	[11]
8	Spent brewery grains	24.02	[23]
9	Egyptian bagasse pith	17.50	[24]
10	Diatomite	21.41	[25]
11	Peat	12.7	[26]
12	Wood	11.60	[27]
13	Maize cob	41.40	[27]
14	Bagasse pith	21.70	[27]
15	Char from bamboo	16.91	[28]
16	Peat	8.9–16.3	[29]

6. Comparison of various low-cost adsorbents

Table 5 presents the biosorption capacity of BGFS for the removal of AB25 dye from aqueous solution. The capacity of BGFS for dye removal substantially compared with other sorbents. The results showed that the biosorption capacity of BGFS for AB25 in the absence and in presence of CTAB is 29.4 and 166.6 mg g^{-1}, respectively. In the presence of CTAB, the biosorption capacity of BGFS (BGFS-CTAB) was the highest among the low-cost adsorbents for AB25 reported earlier (Table 4) [11,23–29]. It can be concluded that BGFS-CTAB is more efficient for the removal of AB25 from aqueous solutions when compared with the effectiveness of other adsorbents.

7. Conclusion

The biosorbent BGFS has been proven as a potential material for the removal of AB25 dye, and the biosorption processes was temperature dependent. The BGFS-CTAB exhibited the highest sorption capacity for AB25 removal when compared with previously reported data in the literature.

- The presence of 0.9 mmol L^{-1} of CTAB in a BGFS-AB25 medium substantially increased the biosorption capacity from 29.4 mg g^{-1} (in the absence of CTAB) to 166.6 mg g^{-1} (in the presence of CTAB).
- The pseudo-second-order model described the biosorption process better than the pseudo-first-order model. Intra-particle diffusion played a major role at the initial stage of the sorption process.
- The Langmuir isotherm described the biosorption data more better than the Freundlich isotherm in the presence of a surfactant.
- The biosorption process conformed to the monolayer, and the values of the maximum biosorption capacities (q_e) was calculated from the Langmuir model were closer to the experimental values of q_e.
- The biosorption process was spontaneous and exothermic as shown by thermodynamic parameters. The values of free energy ($\Delta G°$) suggested that the biosorption was a physical sorption process. This observation signifies that the CTAB enhanced AB25 uptake, and therefore BGFS-CTAB is a promising and potential sorbent system for removal of dyes from aqueous solutions and wastewaters.

Acknowledgements

The authors are grateful to the Universiti Teknologi Malaysia for providing financial support, Post Doc RU Grant (PDRU) VOT 02E94 and also Postdoctoral Fellowship under Rachadapisaek Sompote Fund, The Graduate School, Chulalongkorn University, for financial support and fellowships.

References

[1] M.C.S. Reddy, L. Sivarama Krishna, A.V. Reddy, The use of an agricultural waste material, Jujuba seeds for the removal of anionic dye (Congo red) from aqueous medium, J. Hazard. Mater., 203 (2012) 118–127.
[2] Z. Aksu, Application of biosorption for the removal of organic pollutants: a review, Process. Biochem., 40 (2005) 997–1026.
[3] W. Zhang, H. Li, X. Kan, L. Dong, H. Yan, Z. Jiang, H. Yang, A. Li, R. Cheng, Adsorption of anionic dyes from aqueous solutions using chemically modified straw, Bioresour. Technol., 117 (2012) 40–47.
[4] W.S. Wan Ngah, L.C. Teong, M.A.K.M. Hanafiah, Adsorption of dyes and heavy metal ions by chitosan composites: a review, Carbohydr. Polym., 83 (2011) 1446–1456.
[5] M. Vakili, M. Rafatullah, B. Salamatinia, A.Z. Abdullah, M.H. Ibrahim, K.B. Tan, Z. Gholami, P. Amouzgar, Application of chitosan and its derivatives as adsorbents for dye removal from water and wastewater: a review, Carbohydr. Polym., 113 (2014) 115–130.
[6] J.-S. Cao, J.-X. Lin, F. Fang, M.-T. Zhang, Z.-R. Hu, A new absorbent by modifying walnut shell for the removal of anionic dye: kinetic and thermodynamic studies, Bioresour. Technol., 163 (2014) 199–205.
[7] M.S. Sajab, C.H. Chia, S. Zakaria, S.M. Jani, M.K. Ayob, K.L. Chee, P.S. Khiew, W.S. Chiu, Citric acid modified kenaf core fibres for removal of methylene blue from aqueous solution, Bioresour. Technol., 102 (2011) 7237–7243.
[8] R.P. Han, L. Zhang, C. Song, M. Zhang, H. Zhu, L. Zhang, Modified wheat straw, kinetic and equilibrium study about

copper ion and methylene blue adsorption in batch mode, Carbohydr. Polym., 79 (2010) 1140–1149.
[9] S. Chakraborty, S. Chowdhury, P. Das Saha, Adsorption of crystal violet from aqueous solution onto NaOH-modified rice husk, Carbohydr. Polym., 86 (2011) 1533–1541.
[10] M.S.U. Rehman, I. Kim, J.I. Han, Adsorption of methylene blue dye from aqueous solution by sugar extracted spent rice biomass, Carbohydr. Polym., 90 (2012) 1314–1322.
[11] F. Ferrero, Dye removal by low cost adsorbents: hazelnut shells in comparison with wood sawdust, J. Hazard. Mater., 142 (2007) 144–152.
[12] Y. Wu, H. Luo, H. Wang, C. Wang, J. Zhang, Z. Zhang, Adsorption of hexavalent chromium from aqueous solutions by graphene modified with cetyltrimethylammonium bromide, J. Colloid. Interface. Sci., 394 (2013) 183–191.
[13] F. Wu, R. Tseng, R. Juang, Pore structure and adsorption performance of the activated carbons prepared from plum kernels, J. Hazard. Mater., 69 (1999) 287–302.
[14] C.H. Weng, Y.J. Chen, True color removal from real textile wastewater using waste tea leaf powder, Environ. Eng. Mang. J., 14 (2015) 2383–2391.
[15] C.H. Weng, Y.T. Lin, Y.J. Chen, Y.C. Sharma, Spent green tea leaves for decolourisation of raw textile industry wastewater, Color. Technol., 129 (2013) 298–304.
[16] R. Sanghi, P. Verma, Decolorisation of aqueous dye solutions by low-cost adsorbents: a review, Color. Technol., 129 (2013) 85–108.
[17] C.H. Weng, Y.T. Lin, T.W. Tzeng, Removal of methylene blue from aqueous solution by adsorption onto pineapple leaf powder, J. Hazard. Mater, 170 (2009) 417–424.
[18] L. Sivarama Krishna, A. Yuzir, G. Yuvaraja, V. Ashokkumar, Removal of Acid blue 25 from aqueous solutions by using Bengal gram fruit shell (BGFS) biomass, Int. J. Phytorem., 19 (2017) 431–438.
[19] S. Chatterjee, M.W. Lee, S.H. Wooa, Influence of impregnation of chitosan beads with cetyl trimethyl ammonium bromide on their structure and adsorption of congo red from aqueous solutions, Chem. Eng. J., 155 (2009) 254–259.
[20] B.C. Oei, S. Ibrahim, S. Wang, H.M. Ang, Surfactant modified barley straw for removal of acid and reactive dyes from aqueous solution, Bioresour. Technol., 100 (2009) 4292–4295.
[21] H.Z. Kavas, M. Durmus, S.Şenel, A.K. Baykal, S.T. Muhammet, CTAB-Mn_3O_4 nanocomposites: synthesis, NMR and low temperature EPR studies, Polyhedron, 29 (2010) 1375–1380.
[22] S. Chatterjee, D.S. Lee, M.W. Lee, S.H. Woo, Enhanced adsorption of congo red from aqueous solutions by chitosan hydrogel beads impregnated with cetyl trimethyl ammonium bromide, Bioresour. Technol., 100 (2009) 2803–2809.
[23] V. Jaikumar, K.S. Kumar, D.G. Prakash, Biosorption of acid dyes using spent brewery grains: characterization and modeling, Int. J. Appl. Sci. Eng., 7 (2010) 115–125.
[24] K. Badii, F.D. Ardejani, M.A. Saberi, N.Y. Limaee, Adsorption of Acid blue 25 dye on diatomite in aqueous solutions, Indian J. Chem. Tech.,17 (2010) 7–16.
[25] B. Chen, C.W. Hui,. Mckay, Film-pore diffusion modeling and contact time optimization for the adsorption of dyestuffs on pith, Chem. Eng. J., 84 (2001) 77–94.
[26] Y.S. Ho, G. McKay, Kinetic models for the sorption of dye from aqueous solution by wood, Trans I. Chem. E., 76 (1998) 183–191.
[27] V.K. Gupta, P.J.M. Carrott, M.M.L. Ribeiro Carrott, Low-cost adsorbents: growing approach to wastewater treatment—a review, Crit. Rev. Env. Sci. Tec., 39 (2009) 783–842.
[28] E.L.K. Mui, W.H. Cheung, M. Valix, G. McKay, Dye adsorption onto char from bamboo, J. Hazard. Mater., 177 (2010) 1001–1005.
[29] V.J.P. Poots, G. McKay, J.J. Healy, The removal of acid dye from effluent using natural adsorbents—I peat, Water. Res., 10 (1976) 1061–1066.